STUDY OF THE CONTINUOUS SOLAR SPECTRUM IN THE VISIBLE RANGE

by A. S. RAMANATHAN
(Kodaikanal Observatory, India)

ABSTRACT. — *Limb darkening observations made under excellent observing conditions are given for twenty-two wavelengths in the continuous spectrum of the sun in the region* λ 3 600-λ 6 800 *; these observations were made at a time when the disc was completely free from spots and also other forms of solar activity were at a minimum. It is verified that for the visible region between* λ 4 000 *and* λ 6 000 *the variation of continuous absorption coefficient with wavelength agrees with the theoretical values given by* CHANDRASEKHAR *and* BREEN *for the* H^- *ion. However beyond* 6 000 Å *divergence between theory and observation begins to appear. Variation of optical depth with temperature for* λ 5 000 *is deduced from observations.*

INTRODUCTION

It is well established that the observed energy distribution over wavelengths in the spectrum of the sun, whose effective temperature is 5 713° as deduced from the solar constant, deviates considerably from the Planckian radiation curve for 5 713°. This means that the sun does not radiate strictly like a black body. The main object of any theory of the photosphere is to account for this discrepancy between the effective temperature and the colour temperature and for the observed variation of limb darkening with wavelength. Such a theory, of which the investigation by CHALONGE and KOURGANOFF is a recent example, usually bases itself upon accurate observational data relating to the variation of limb darkening with wavelength and to the variation of intensity as a function of wavelength at the centre of the solar disc or for the disc as a whole. As the thickness of the solar atmosphere is small compared to the radius of the sun, it is important that the measurements of limb darkening required by a photospheric theory, which has to explain the variation of the continuous absorption coefficient, should be extended as close as possible to the extreme limb. Such measurements have been made by several workers [1], of whom ABBOT was the earliest, in the continuous spectrum of the sun extending from the ultraviolet to the infrared. But in recent years greater emphasis seems to have been laid upon measurements in the infrared and the ultraviolet than in the visible part of the solar spectrum. CANAVAGGIA and CHALONGE [2] have however recently studied the darkening towards the solar limb over the spectral range from λ 3 150 to λ 6 000, but they regard their measures to be of the nature of only a first

approximation. There is indeed an urgent need for accurate measurements of limb darkening in the visible region of the solar spectrum and under as perfect observing conditions as possible.

From an analysis of the measurements so far available CHALONGE and KOURGANOFF [3] have come to the conclusion that between λ 4 000 and λ 12 000 the observations are consistent with the hypothesis put forward by WILDT [4] that the negative hydrogen ion is the sole source of opacity in the solar atmosphere, while CHANDRASEKHAR and MÜNCH [5] believe that the agreement between theory and observation is sufficiently good over the whole spectral range from 4 000 Å to 24 000 Å. It is with the object of providing really reliable measurements of the solar limb darkening in the visible region and with the view of examining how far the theory of absorption by the H^-ion agrees with observations made under the best possible conditions that the present work was undertaken.

OBSERVATIONS OF LIMB DARKENING

Experimental details. — Limb darkening observations in the wavelength range λ 3 600-λ 6 800 were carried out with the help of a plane grating spectrograph in angular mounting fed by an 18-inch Foucault siderostat and an 8-inch achromatic object glass of about 9 1/2 feet focal length giving a solar image of about 28 mm in diameter. The grating is ruled on speculum and the collimator and the camera objectives are of glass. Further details about the spectrograph are given in [6].

The spectrograms were obtained in the second order of the grating, where the linear dispersion was 2 Å per millimeter and also partly in the first order where the scale of the spectrum was half that in the second order. From 3 600 Å to 5 300 Å the spectrum was photographed in the second order, while for the range from 5 300 Å to 6 800 Å the first order of the grating was used. Thus there was no need to use colour filters for eliminating the effect of overlapping spectra. The experimental procedure was as follows: the image of the sun was guided on to the slit plate so as to place it symmetrically on the slit which was about 0,04 mm in width and 32 mm in effective length. With the help of a metal disc placed immediately in front of the slit and having a circle of about 28 mm in diameter engraved on it, the focussed image was centred upon the slit so that the vertical diameter of the image exactly coincided with the slit. The focussing of the image on the slit plate was made visually always by looking through a colour filter appropriate to the particular region for which the spectrograph was adjusted. With this arrangement spectrograms were taken in the various regions of the spectrum covering the entire visible part. Thus on the plates were obtained spectra of the focussed diameter of the sun's image. The exposures were quite short varying between 2 and 7 seconds. The whole visible region was photographed in eight

sections and in each section several plates were obtained on several days in the months of December and January 1952-1953 when the observing conditions were exceptionally good and the disc of the sun was completely free from spots. The photographic plates (8 1/2″ × 6 1/2″) used were Ilford Process for the region 3 600 Å-4 500 Å, Ilford Selochrome for the region 4 600 Å-5 000 Å, Ilford Special Rapid Panchromatic for the region 5 000-Å-6 000 Å and Ilford Astra VIII for the region 6 000 Å-6 800 Å. The whole range of wavelengths between λ 3 600 and λ 6 800 photographed covered about 1 225 mm. All the plates were developed in total darkness for 5 minutes in M. Q. developer taking the usual precautions to eliminate EBERHARD effect. Each plate contained one spectrum of the sun as well as a series of density marks for determining its characteristic curve. The procedure for obtaining the density marks was as follows : the slit of the spectrograph was opened to its fullest extent of about 2,5 mm and a previously calibrated step slit was placed at a fixed distance immediately in front of it. The details of the procedure for impressing the density marks on the plates are described in [6]. It was found that an exposure varying between 5 and 20 seconds gave suitable densities with the step slit for microphotometry in all the regions, while the exposure times for the solar spectrum varied between 2 and 7 seconds. Thus the ratio between the time of exposure for the solar spectrum and that for the density marks was never more than three. For this ratio, it was assumed that the characteristic curve of the photographic plate is not affected. In order to keep this ratio always less than three a high quality Kodak Neutral Filter was used behind the slit when the solar spectra were taken and removed while taking the standardisation spectra.

REDUCTION OF OBSERVATIONS

The spectra obtained represent the spectra of the focussed diameter of the sun's image extending from one limb to the other and can therefore be used for measurements of limb darkening for various wavelengths in the continuous spectrum. A determination of the variation of intensity in the continuous spectrum parallel to the Fraunhofer lines is intended to give the variation of intensity from limb to limb along a diameter of the solar disc for the particular wavelengths under consideration. This requires that two important conditions should be fulfilled : (*a*) that the spectrograph slit is absolutely uniform in width throughout its length so that whatever variation is measured along the spectrum is entirely due to limb darkening, (*b*) that the spectrograph is completely free from astigmatism. As regards (*a*) the slit, although of excellent construction, was carefully tested for uniformity of breadth by photographing the spectrum in some spectral region with the slit illuminated by uniform unfocussed sun light. The spectrogram was then run through a recording microphotometer across the conti-

nuum in a direction parallel to the Fraunhofer lines. This showed that the slit jaws were perfectly straight, but the slit width had a very slight uniform taper from one end to the other, which made the intensity of the spectrum decrease uniformly along the length of the slit. While it could be completely eliminated for any fixed width of the slit, this tapering could not be entirely avoided when the slit had to be opened and closed several times for photographing the standardisation spectra on the different plates. However, this had no objectionable influence on the results, for by taking corresponding points on either side of the centre of the image and averaging, the real intensity for each point could be correctly determined. In actual measurement corresponding points on either side of the centre were found to differ utmost by about 6 %, though in many cases the difference was much less. So far as condition (*b*) is concerned, various tests were made for detecting signs of astigmatism, but the spectrograph appeared to be completely free from this defect.

TABLE I

Values of $\frac{I_\lambda(0,\theta)}{I_\lambda(0,0)}$ *for various wavelengths in the visible region.*

λ in A° \ Sin θ	0	0.2	0.3	0.4	0.5	0.6	0.7	0.8	0.85	0.9	0.95	0.98
3 600	1.000	.987	.975	.947	.908	.853	.782	.676	.608	.527	.409	.287
3 623	1.000	.989	.973	.950	.921	.873	.794	.705	.639	.557	.448	.315
3 659	1.000	.995	.978	.954	.915	.868	.799	.714	.667	.594	.497	.349
3 692	1.000	.992	.974	.947	.914	.870	.805	.712	.646	.572	.460	.339
3 714	1.000	.988	.976	.953	.924	.884	.831	.741	.679	.596	.468	.345
3 726	1.000	.991	.976	.952	.920	.881	.823	.730	.656	.582	.458	.327
4 094	1.000	.989	.976	.962	.931	.902	.851	.779	.726	.653	.556	.468
4 221	1.000	.982	.963	.943	.917	.875	.818	.746	.698	.632	.546	.453
4 485	1.000	.991	.973	.950	.914	.886	.849	.777	.734	.667	.582	.490
4 532	1.000	.990	.979	.958	.938	.910	.869	.816	.765	.705	.610	.505
4 753	1.000	.988	.977	.962	.939	.909	.870	.815	.769	.709	.622	.515
4 830	1.000	.992	.978	.961	.940	.911	.868	.807	.764	.710	.625	.530
4 995	1.000	.989	.976	.961	.940	.914	.864	.796	.750	.687	.600	.504
5 078	1.000	.993	.979	.963	.939	.908	.866	.805	.760	.713	.634	.555
5 190	1.000	.989	.975	.954	.927	.895	.853	.794	.755	.706	.630	.537
5 305	1.000	.989	.978	.963	.942	.915	.877	.820	.778	.736	.652	.546
5 339	1.000	.989	.980	.963	.943	.912	.872	.810	.771	.708	.623	.533
5 500	1.000	.995	.991	.979	.966	.944	.912	.858	.820	.760	.676	.591
5 750	1.000	.994	.989	.980	.966	.946	.916	.865	.825	.768	.681	.588
6 210	1.000	.997	.985	.965	.944	.923	.895	.853	.828	.779	.712	.637
6 397	1.000	.994	.983	.973	.961	.945	.922	.894	.870	.830	.757	.657
6 670	1.000	.992	.981	.969	.963	.942	.915	.882	.862	.827	.771	.692

The plates were taken only in the early hours of the morning when the observing conditions at Kodaikanal are at their best. Although about 100 plates were actually taken a selection for correct density for microphotometry had to be made. The plates finally chosen were 30 in number ; these were photometered with a Cambridge Recording Microphotometer. About thirty wavelengths in all were chosen where there was a good continuous spectrum seemingly free from the influence of strong absorption lines. Careful comparison with the Utrecht Photometric Atlas however showed that a few of these wavelengths were not entirely free from the influence of Fraunhofer lines and were therefore rejected. The final measurements reported in the present paper give the values of limb darkening for 22 wavelengths. Three independent limb darkening curves were prepared for each wavelength and in each case the intensities at points .2, .3, .4, .5, .6, .7, .8, .85, .9, .95 and .98 radius from the centre on either side were measured, averaged for corresponding points on both sides and expressed as fractions of the intensity at the centre. The three curves for each wavelength gave quite consistent values which agreed within 2 %. The averages for each wavelength are collected in Table I.

DEFINITION OF THE LIMB AND SOURCES OF ERROR

Under the conditions in which the spectrograms were secured, the definition of the sun's image was excellent. Accordingly the spectrum lines showed fine definition, except in the region 3 600 Å-3 800 Å, where the definition of the spectrum was somewhat impaired due to the presence of appreciable diffuse light inside the spectrograph. The repetition of the measurements in the region 3 600 Å-3 800 Å and its extension to the limit of the ozone band using a prism spectrograph is contemplated.

One important source of error is the blurring of the solar image due to scintillation and scattering in the atmosphere. According to MINNAERT and his coworkers [7], due to the diffusion of the sun's limb, each point along a solar radius is blurred according to a Gaussian curve,

$$j = \frac{a}{\pi} e^{-(\xi^2+\eta^2)a}$$

where ξ and η are cartesian coordinates in units of solar radius, measured in the direction of and normal to the solar radius. This assumption is essentially the same as that of WANDERS [8]. The quantity ' a ' called scintillation constant is very large when diffusion effects are very small. Assuming that the limb is really a straight edge, the effect of the diffusion process will be to distort the intensity profile into an S-shaped curve. The position of the true limb is at the point

of inflection of the curve. A family of theoretical curves can be constructed with parameter ' a ', so that by comparing the observational curves with the theoretical curves one can determine the scattering constant ' a ', which can be used to determine the true intensities near the limb. Estimates of ' a ' were thus made for all the observational curves and it was found that while in the region 4 000 Å-4 500 Å ' a ' varied between 28 000 and 50 000 the variation was between 80 000 and 110 000 for wavelengths above 4 500 Å. There was considerable blurring in the region 3 600 Å-3 800 Å and estimates of ' a ' here varied between 3 000 and 10 000.

Another source of distortion of the solar image is the image-forming lens. The actual lens used in our observations is however a high-quality telescope objective constructed by GRUBB and its contribution to the blurring of the image can be taken to be very small (*).

The spectrograph used in this work was provided with several diaphragms with a view to reducing stray light to a minimum. The spectrum plates actually showed extremely faint backgrounds over the whole range photographed, excepting in the range 3 600 Å-3 800 Å where the background was appreciable. The presence of scattered light inside the spectrograph can affect limb darkening measurements. In our measurements a correction for background was made for every plate.

Since in most of the cases the estimates of scintillation constant was very large, it is evident that the effect of scintillation is very small and hence the correction due to diffusion is generally negligible. Since the error introduced by a scintillation constant 30 000 at $\sin\theta = .98$ is about 0.1 %, it was considered safe to carry out the measurements upto $\sin\theta = .98$, without correction for diffusion. The position of the true limb was determined in each case by locating the point of inflection of the S curve. A number of trial cases showed that the point of inflection of the S density curve is the same as the point of inflection of the S intensity curve. This is due to the fact that the diffusion effect has been small throughout.

COMPARISON WITH OTHER OBSERVERS

An examination of the results here reported shows that our values are consistently higher than the values of any other previous observer. This disagreement is to be traced to the method of measurement used by us. The procedure followed

(*) The observations of the limb darkening were first made under equally good observing conditions, using the same spectrograph, but a different image-forming system, viz. an 18-inch parabolic mirror of about 10 ft. focal length. But these showed excessive limb darkening which was evidently due to the vignetting of the solar image caused by the parabolic mirror and the Cassegrain arrangement.

by other observers is such that, for the registration of intensity, they had to bring in succession different points on the sun's diameter on to the registering apparatus, which necessarily involved uncertainties arising from possible changes in observing conditions or from imperfect guiding of the solar image or from both. But the method which we have followed is free from such uncertaintes, because the spectrum of the whole diameter of the sun is recorded all at once in a very short interval of the order of 2 to 7 seconds. In this procedure, therefore, there is far less chance of the relative values of the intensities at different points on the diameter being affected. Incidentally, it may be noted that our observations in the λ 3 600 region agree nearly with the values given by CHALONGE and CANAVAGGIA for the wavelengths in this region. In our case there was considerable diffuse light inside the spectrograph and also the limb profiles showed that considerable correction was necessary for the intensities near the limb. In view of our results obtained by a method which seems freer from the uncertainties indicated above, it seems justified to conclude that the true limb darkening is less than what others have observed.

DISCUSSION OF THE OBSERVATIONS

CHALONGE and KOURGANOFF have worked out a method for determining the variation of the optical depth (τ_λ) in the sun's atmosphere as a function of the wavelength λ, — a method which has been used by a number of later workers. This procedure depends upon two types of observational data, namely (*a*) measures of limb darkening for various wavelengths, and (*b*) measures of intensity as a function of the wavelength at the centre of the disc. In the preceding parts of the present paper we have made a fresh determination of (*a*) in the visible part of the solar spectrum under the best possible conditions. It is also our intention to determine (*b*) under equally satisfactory conditions, but so far, for various reasons, it has not been possible to accomplish this. For the present therefore we accept the intensity distribution in the continuous spectrum between the Fraunhofer lines as a function of wavelength at the centre of the disc as derived by MULDERS from various comparatively recent observations. Although later studies have shown that MULDERS's intensity distribution is considerably in error in the ultraviolet and the infrared parts of the spectrum, his values are satisfactory in the visible range (*).

We follow CHALONGE and KOURGANOFF's procedure for determining the

(*) More recent observations of the absolute intensity distribution at the centre of the disc are however available from the work of CANAVAGGIA and CHALONGE [2]. But they cover only a small range λ 4 000-λ 4 900 in the visible region. In any case these values do not differ materially from those of Mulders, (*Zs. f. Ap.*, 11, 132, 1936.)

variation of τ_λ with λ, using our measures of the darkening towards the limb in the visible range between 4 000 Å and 6 600 Å and MULDERS's intensity distribution at the centre of the disc for the same spectral range. We start with the usual expression

$$I_\lambda(0,\theta) = \int_0^\infty B_\lambda(\tau_\lambda)\, e^{-\tau_\lambda \sec\theta}.\sec\theta\, d\tau_\lambda \quad \ldots. \tag{1}$$

where $d\tau_\lambda = k_\lambda \rho dx$, k_λ = coefficient of continuous absorption and ρ = density. $B_\lambda(\tau_\lambda)$ is the PLANCK function for the temperature corresponding to τ_λ. Now, in actual limb darkening observations we measure the quantity

$$\Phi_\lambda(\theta) = \frac{I_\lambda(0,\theta)}{I_\lambda(0,0)} \quad \ldots. \tag{2}$$

Therefore from (1) and (2) we obtain

$$\Phi_\lambda(\theta) = \int_0^\infty b_\lambda(\tau_\lambda)\, e^{-\tau_\lambda \sec\theta}.\sec\theta\, d\tau_\lambda \quad \ldots. \tag{3}$$

in which

$$b_\lambda(\tau_\lambda) = \frac{B_\lambda(\tau_\lambda)}{I_\lambda(0,0)} \quad \ldots. \tag{4}$$

Various representations have been tried by different writers for $b_\lambda(\tau_\lambda)$. CHALONGE and KOURGANOFF [3] assumed that it could be expressed in the form

$$b_\lambda(\tau_\lambda) = \alpha_\lambda + \beta_\lambda \tau_\lambda + \frac{1}{2}\gamma^\lambda \tau^{\lambda_2} \quad \ldots. \tag{5}$$

which means that

$$\Phi_\lambda(\theta) = \alpha_\lambda + \beta_\lambda \cos\theta + \gamma_\lambda \cos^2\theta \quad \ldots. \tag{6}$$

It is possible to determine α_λ, β_λ and γ_λ by the method of least squares for each wavelength for which limb darkening observations are available. Making use of these coefficients, it can be seen how far the assumed empirical formula faithfully represents the limb darkening curve. In principle, one is not justified in limiting the series upto only three terms. It is necessary to include terms of higher powers of cos θ and evaluate their coefficients by the method of least squares. But nevertheless the formula (6) will remain an interpolation formula and may not hold good for large optical depths due to inaccuracies in observation.

KOURGANOFF [9] has proposed another empirical expression for $b_\lambda(\tau_\lambda)$ which may be written as

$$b_\lambda(\tau_\lambda) = A_\lambda + B_\lambda \tau_\lambda + C_\lambda E_2(\tau_\lambda) + D_\lambda E_3(\tau_\lambda) + \ldots. \tag{7}$$

where A_λ, B_λ, C_λ etc. are empirical constants to be determined for each wavelength from the limb darkening observations and $E_2(\tau_\lambda)$, $E_3(\tau_\lambda)$ etc... are the exponential integrals defined by

$$E_n(x) = \int_1^\infty y^{-n} e^{-xy}\, dy \quad \ldots. \tag{8}$$

Substituing (7) in equation (3) we get

$$(9)\quad \Phi_\lambda(\theta) = A_\lambda + B_\lambda \mu + C_\lambda \left[1 - \mu \log_e \left(1 + \frac{1}{\mu}\right)\right] + D_\lambda \left[\frac{1}{2} - \mu + \mu^2 \log_e \left(1 + \frac{1}{\mu}\right)\right] + \ldots.$$

where $\mu = \cos\ \theta$.

In order to decide which of the two representations (5) and (7) fits better with the observations three different wavelengths were chosen in the entire region investigated and for these three wavelengths the coefficients were evaluated first in (5) and then in (7) by the method of least squares, and the sums of squares of residuals were computed in both cases for these three wavelengths. The results are given in the table II, an examination of which shows that the representation (7) is much superior to (5).

TABLE II

λ	Σe^2 FOR (5) UPTO THREE TERMS	Σe^2 FOR (7) UPTO THREE TERMS
4 221 Å	.00009333	.00006150
5 190 Å	.00032516	.00013115
6 397 Å	.00098978	.00023680

Accordingly the representation (7) was chosen and the coefficients A_λ, B_λ and C_λ in (7) for each wavelength finally evaluated by the method of least squares are given in table III, correct to 6 decimal places.

TABLE III

Values of the coefficients A_λ, B_λ, C_λ *in* (7).

λ IN Å	A_λ	B_λ	C_λ	$A_\lambda + C_\lambda$
4 094	0.795589	0.407953	— 0.648039	0.147550
4 221	0.556468	0.540680	— 0.328139	0.228329
4 485	0.740157	0.414560	— 0.519293	0.220864
4 532	1.045408	0.234330	— 0.916613	0.128795
4 753	1.018700	0.242130	— 0.858392	0.160308
4 830	0.898535	0.306925	— 0.669678	0.228857
4 995	0.881561	0.335244	— 0.696688	0.184873
5 078	0.741962	0.386176	— 0.412198	0.329764
5 190	0.741703	0.385659	— 0.431464	0.310239
5 305	1.006890	0.229873	— 0.783411	0.223479
5 339	0.911871	0.300800	— 0.687516	0.224355
5 500	1.161714	0.134552	— 0.941008	0.220706
5 750	1.254201	0.064842	— 1.031074	0.223127
6 210	0.955283	0.212154	— 0.559736	0.395547
6 397	1.355158	— 0.035758	— 1.069778	0.285380
6 670	1.084631	0.105123	— 0.637799	0.446832

If we put $\theta = \frac{\pi}{2}$ in equation (9), we get the limb intensity $\Phi_\lambda\left(\frac{\pi}{2}\right) = A_\lambda + C_\lambda$, expressed in terms of the intensity at the centre. Taking MULDERS' values for the intensity at the centre of the disc it is possible to obtain $I_\lambda\left(0, \frac{\pi}{2}\right)$ at the extreme limb $[(A_\lambda + C_\lambda)\ (I_\lambda(0, 0)]$ and hence the boundary temperature of the sun. Different writers have obtained different values for this temperature. Our observations yield the value 4 793° ± 125°. In the calculations which follow we therefore adopt 4 800° as the boundary temperature. Table IV gives the boundary temperatures obtained for different wavelengths (1).

TABLE IV

Boundary temperature. — T_0

λ IN Å	T_0(°K)	IN Å	T_0(°K)	
4 094	4 779	5 190	4 997	
4 221	5 057	5 305	4 683	
4 485	4 951	5 339	4 675	
4 532	4 555	5 500	4 614	
4 753	4 622	5 750	4 555	
4 830	4 859	6 210	4 984	
4 995	4 637	6 397	4 615	
5 078	5 086	6 670	5 026	Mean = 4 793° ± 125°

DÉTERMINATION OF $b_\lambda(\tau_\lambda)$

Once A_λ, B_λ and C_λ are determined for each wavelength, it is easy to calculate $b_\lambda(\tau_\lambda)$ with the aid of the equation (7) with 3 terms for various values of τ_λ and for different wavelengths. Tables of $E_2(\tau)$ for various values of τ_λ are available from KOURGANOFF's book [10] on *Transfer Problems*, which we have made use of in evaluating $b_\lambda(\tau_\lambda)$. The results are given in table V. Since $b_\lambda(\tau_\lambda) = \frac{B_\lambda(\tau_\lambda)}{I_\lambda(0, 0)}$ it is now possible to determine $B_\lambda(\tau_\lambda)$ for each wavelength and for different values of τ_λ and hence the temperature distribution with optical depth for each wavelength. The values of T as a function of τ_λ and λ are assembled in table VI. Then the temperatures thus obtained are plotted against τ_λ for various wavelengths. From these curves it is possible now to read off τ_λ for each wavelength for some chosen temperatures. We have chosen the temperatures 5 000°, 5 500°, 6 000°, 6 500° and 7 000° and for these, τ_λ's for all the wavelengths are read off. These values are assembled in table VIII. Then τ_λ is plotted against λ for all the chosen temperatures (fig. 2).

(1) It is well known that the true surface temperature is lower.

TABLE V

Values of $b_\lambda(\tau_\lambda)$ for different λ's and τ_λ's

τ_λ \ λ	4 094	4 221	4 485	4 532	4 753	4 830	4 995	5 078	5 190	5 305	5 339	5 500	5 750	6 210	6 397	6 670
—	—	—	—	—	—	—	—	—	—	—	—	—	—	—	—	—
0.00	0.14755	0.22833	0.22087	0.12880	0.16031	0.22886	0.18487	0.32976	0.31024	0.22348	0.22435	0.22070	0.22313	0.39555	0.28538	0.44683
0.02	0.21201	0.26766	0.27428	0.21312	0.23973	0.29319	0.25210	0.37329	0.35545	0.29614	0.29012	0.30515	0.31402	0.44843	0.37770	0.50436
0.05	0.27951	0.31186	0.33098	0.29830	0.32017	0.35948	0.32155	0.42003	0.40380	0.36983	0.35773	0.38940	0.40404	0.50251	0.46780	0.56189
0.08	0.33509	0.35003	0.37817	0.36666	0.38488	0.41351	0.37824	0.45919	0.44424	0.42915	0.41276	0.45663	0.47480	0.54632	0.53830	0.60772
0.10	0.36812	0.37345	0.40640	0.40653	0.42266	0.44534	0.41168	0.48273	0.46851	0.46481	0.44518	0.49523	0.51568	0.57205	0.57865	0.63430
0.20	0.50506	0.47621	0.52488	0.56596	0·57423	0.57539	0.54858	0.58252	0.57109	0.60303	0.57725	0.64828	0.67513	0.67630	0.73379	0.73944
0.40	0.70642	0.64497	0.70378	0.78223	0.78130	0.76055	0.74438	0.73593	0.72796	0.79380	0.76448	0.84912	0.87865	0.82219	0.92434	0.87834
0.60	0.86138	0.79025	0.84547	0.93285	0.92690	0.89774	0.89028	0.85983	0.85394	0.92844	0.90247	0.98254	1.00833	0.92797	1.03825	0.97156
0.80	0.99179	0.92311	0.96734	1.04878	1.04000	1.00960	1.00982	0.96813	0.96358	1.03345	1.01443	1.08036	1.09900	1.01258	1.11171	1.04063
1.00	1.10730	1.04842	1.07758	1.14362	1.13335	1.10602	1.11333	1.06703	1.06329	1.12042	1.11057	1.15651	1.16592	1.08431	1.16055	1.09504
1.25	1.23846	1.19836	1.20461	1.24345	1.23252	1.21299	1.22851	1.18203	1.17913	1.21315	1.21670	1.23251	1.22854	1.16254	1.19975	1.15002
1.50	1.36015	1.34350	1.32404	1.32990	1.31925	1.30998	1.33349	1.29119	1.27865	1.29443	1.31281	1.29474	1.27608	1.23259	1.22332	1.19569
1.75	1.47569	1.48554	1.43855	1.40767	1.39765	1.40072	1.43188	1.39626	1.39409	1.36829	1.40240	1.34808	1.31388	1.29734	1.23677	1.23533
2.00	1.58717	1.62539	1.54979	1.47966	1.47074	1.48726	1.52589	1.49885	1.49682	1.43723	1.48766	1.39549	1.34518	1.35857	1.24349	1.27094
2.25	1.69586	1.76408	1.65880	1.54773	1.54015	1.57093	1.61691	1.59966	1.59771	1.50280	1.56998	1.43887	1.37206	1.41740	1.24562	1.30382
2.50	1.80264	1.90767	1.76628	1.61309	1.61703	1.65260	1.70587	1.69925	1.69731	1.56606	1.65026	1.47945	1.39589	1.47458	1.24458	1.33481
2.75	1.90806	2.03859	1.87268	1.67654	1.67206	1.73289	1.79338	1.79798	1.79601	1.62768	1.72911	1.51809	1.41757	1.53059	1.24132	1.36448
3.00	2.01254	2.17502	1.97831	1.73865	1.73595	1.81220	1.87987	1.89611	1.89409	1.68816	1.80695	1.55532	1.43775	1.58577	1.23650	1.39321
3.50													1.47516			1.44886
5.00													1.57737			1.60961

TABLE VI

Values of T for various λ's and τ_λ's

τ_λ/λ	4 094	4 221	4 485	4 532	4 753	4 830	4 995	5 078	5 190	5 305	5 339	5 500	5 750	6 210	6 397	6 670
—	—	—	—	—	—	—	—	—	—	—	—	—	—	—	—	—
0.00	4 779	5 057	4 951	4 555	4 622	4 859	4 637	5 086	4 997	4 683	4 675	4 614	4 555	4 894	4 615	5 028
0.02	5 027	5 179	5 122	4 909	4 924	5 063	4 880	5 201	5 122	4 921	4 892	4 893	4 856	5 121	4 893	5 170
0.05	5 233	5 302	5 280	5 177	5 167	5 245	5 089	5 316	5 241	5 118	5 085	5 125	5 104	5 251	5 130	5 305
0.08	5 378	5 399	5 398	5 356	5 334	5 377	5 239	5 406	5 341	5 274	5 225	5 290	5 276	5 351	5 297	5 407
0.10	5 457	5 454	5 464	5 452	5 423	5 449	5 320	5 458	5 396	5 357	5 303	5 377	5 369	5 408	5 388	5 465
0.20	5 738	5 675	5 712	5 779	5 736	5 716	5 617	5 661	5 611	5 645	5 586	5 689	5 695	5 624	5 706	5 681
0.40	6 070	5 975	6 026	6 139	6 090	6 040	5 969	5 936	5 898	5 984	5 929	6 040	6 052	5 899	6 054	5 944
0.60	6 284	6 195	6 239	6 355	6 305	6 246	6 198	6 135	6 104	6 196	6 150	6 247	6 258	6 083	6 244	6 109
0.80	6 449	6 375	6 406	6 507	6 458	6 401	6 368	6 295	6 268	6 350	6 317	6 390	6 391	6 222	6 361	6 227
1.00	6 579	6 529	6 547	6 623	6 578	6 528	6 507	6 432	6 409	6 470	6 452	6 495	6 488	6 335	6 437	6 315
1.25	6 719	6 697	6 698	6 739	6 699	6 662	6 654	6 583	6 564	6 593	6 594	6 598	6 575	6 455	6 498	6 405
1.50	6 841	6 853	6 832	6 836	6 800	6 778	6 780	6 719	6 690	6 698	6 716	6 680	6 639	6 559	6 532	6 477
1.75	6 950	6 994	6 954	6 920	6 889	6 881	6 894	6 844	6 831	6 788	6 827	6 748	6 690	6 653	6 553	6 539
2.00	7 051	7 124	7 066	6 995	6 967	6 977	6 999	6 962	6 950	6 871	6 928	6 807	6 732	6 739	6 563	6 593
2.25	7 146	7 245	7 172	7 064	7 042	7 065	7 097	7 073	7 064	6 948	7 024	6 861	6 767	6 821	6 566	6 645
2.50	7 235	7 363	7 273	7 129	7 121	7 151	7 190	7 179	7 172	7 021	7 114	6 910	6 797	6 899	6 564	6 690
2.75	7 320	7 475	7 369	7 190	7 177	7 231	7 280	7 281	7 277	7 091	7 201	6 956	6 826	6 973	6 559	6 734
3.00	7 401	7 581	7 463	7 250	7 241	7 310	7 365	7 380	7 376	7 157	7 285	7 004	6 851	7 045	6 552	6 777
3.50													6 897			6 858
5.00													7 024			7 084

ROLE OF NEGATIVE HYDROGEN ION

The curves plotted in fig. 2 have now to be compared with the curves that can be obtained by making use of CHANDRASEKHAR's values for the absorption coefficients for the H^- ion. We again follow here the method first suggested by CHALONGE and KOURGANOFF [3]. Let us suppose that the H^- ion is the only absorbent in the wavelength region considered. Then if $k_\lambda(T)$ be the absorption coefficient of the H^- ion given by CHANDRASEKHAR and BREEN [11],

$$\tau_\lambda = \int k_\lambda \rho dx = \int k_\lambda \left(\rho \frac{dx}{dT}\right) dT = \int k_\lambda a_T dT \ldots . \tag{10}$$

where a_T is a coefficient depending only on T.

Differentiating (10) we have

$$\frac{d\tau_\lambda}{dT} = a_T k_\lambda(T) \ldots . \tag{11}$$

Therefore, plotting $\frac{d\tau_\lambda}{dT}$ against $k_\lambda(T)$, we should obtain a straight line passing through the origin and having a slope a_T, if H^- ion is the only source of continuous absorption in the region considered.

TABLE VII

Values of Empirical τ_λ's for various temperatures.

λ/T°(K)	5 000	5 500	6 000	6 500	7 000
—	—	—	—	—	—
4 094	.015	.113	.355	.870	1.880
4 221		.120	.415	.950	1.755
4 485	.005	.110	.380	.930	1.845
4 532	.018	.110	.313	.780	2.000
4 753	.035	.120	.355	.855	2.120
4 830	.010	.110	.375	.950	2.040
4 995	.040	.150	.420	.990	2.000
5 078		.110	.465	1.120	2.075
5 190		.140	.490	1.140	2.100
5 305	.030	.145	.412	1.050	2.425
5 339	.030	.155	.455	1.070	2.180
5 500	.035	.135	.370	1.020	2.500
5 750	.035	.140	.355	1.030	4.650
6 210		.135	.500	1.350	2.850
6 397	.030	.128	.365	1.250	
6 670		.115	.460	1.610	4.440

We have determined $\frac{d\tau_\lambda}{dT}$ for different temperatures from the τ_λ versus T curves and have plotted these values against k_λ given by CHANDRASHEKHAR and BREEN. The temperatures chosen are 5 000°, 5 250°, 5 500°, 5 750°, 6 000°, 6 250°, 6 500°, 6 750°, and 7 000°. The graphs are shown in fig. 1. An exami-

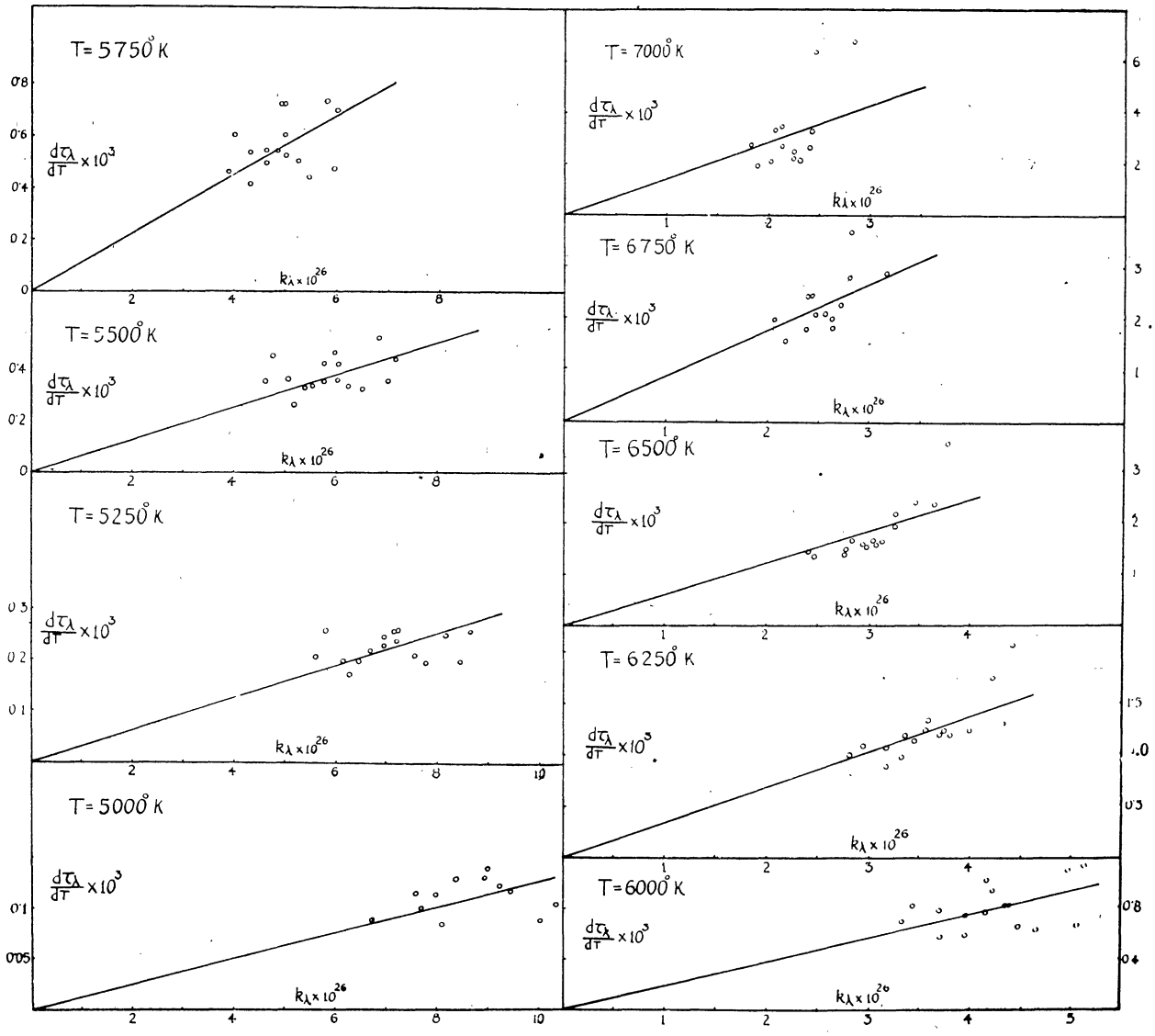

FIG. 1. — Determination of the coefficient a_T for different temperatures.

nation of these graphs shows that there is a certain amount of scatter in the plots, presumably due to uncertainties in the observations. Nevertheless, the best curve that could be drawn was clearly a straight line passing through the origin. From these graphs the best value of a_T was determined in every case. These values are collected in table VIII.

TABLE VIII

T°(K)	5 000	5 250	5 500	5 750	6 000	6 250	6 500	6 750	7 000
a_T X 10^{-23}	.01273	.03112	.06352	.11274	.18834	.34233	.61750	.89189	1.4308

We use the relation

$$\tau_\lambda(T) = \int_{T_0}^{T} a_T k_\lambda(T)\, dT$$

for calculating the optical depth of a layer of temperature T in an atmosphere where absorption is uniquely due to the H^- ion. We adopt $T_0 = 4\,800^o$ K. We have performed the integration of the equation mentioned above graphically after plotting $a_T k_\lambda$ against temperature for various wavelengths. Hence we get the variation of $\tau_\lambda(T)$ with wavelength for various chosen temperatures. The values are assembled in Table IX. We have chosen again the same temperatures viz. 5 000°, 5 500°, 6 000°, 6 500°, and 7 000°, so that we can compare these synthetic curves with the empirical curves obtained from observations. In fig. 2 *o's* represent the empirical plots and X*'s* represent the synthetic plots. An examination of the figure shows that the curves follow one another fairly closely and therefore indicate that the H^- ion is the only source of continuous absorption in

TABLE IX

Values of synthetic τ_λ's for various temperatures.

λ/T°K	5 000	5 500	6 000	6 500	7 000
4 094	0.008	0.099	0.324	0.802	1.750
4 221	0.008	0.097	0.326	0.835	1.831
4 485	0.008	0.102	0.351	0.903	1.985
4 532	0.008	0.104	0.346	0.898	1.987
4 753	0.008	0.109	0.373	0.937	2.038
4 830	0.008	0.116	0.382	0.957	2.098
4 995	0.009	0.121	0.395	0.993	2.169
5 078	0.010	0.121	0.400	1.023	2.215
5 190	0.009	0.122	0.405	1.031	2.265
5 305	0.010	0.123	0.416	1.069	2.344
5 339	0.011	0.127	0.411	1.054	2.315
5 500	0.012	0.133	0.430	1.087	2.386
5 750	0.012	0.137	0.445	1.124	2.474
6 210	0.012	0.149	0.483	1.219	2.671
6 397	0.013	0.150	0.489	1.224	2.703
6 670	0.013	0.153	0.495	1.250	2.746.

the visible range of wavelengths from 4 000 Å to 6 000 Å. The observational curves, however, indicate that beyond 6 000 Å the divergence between theory

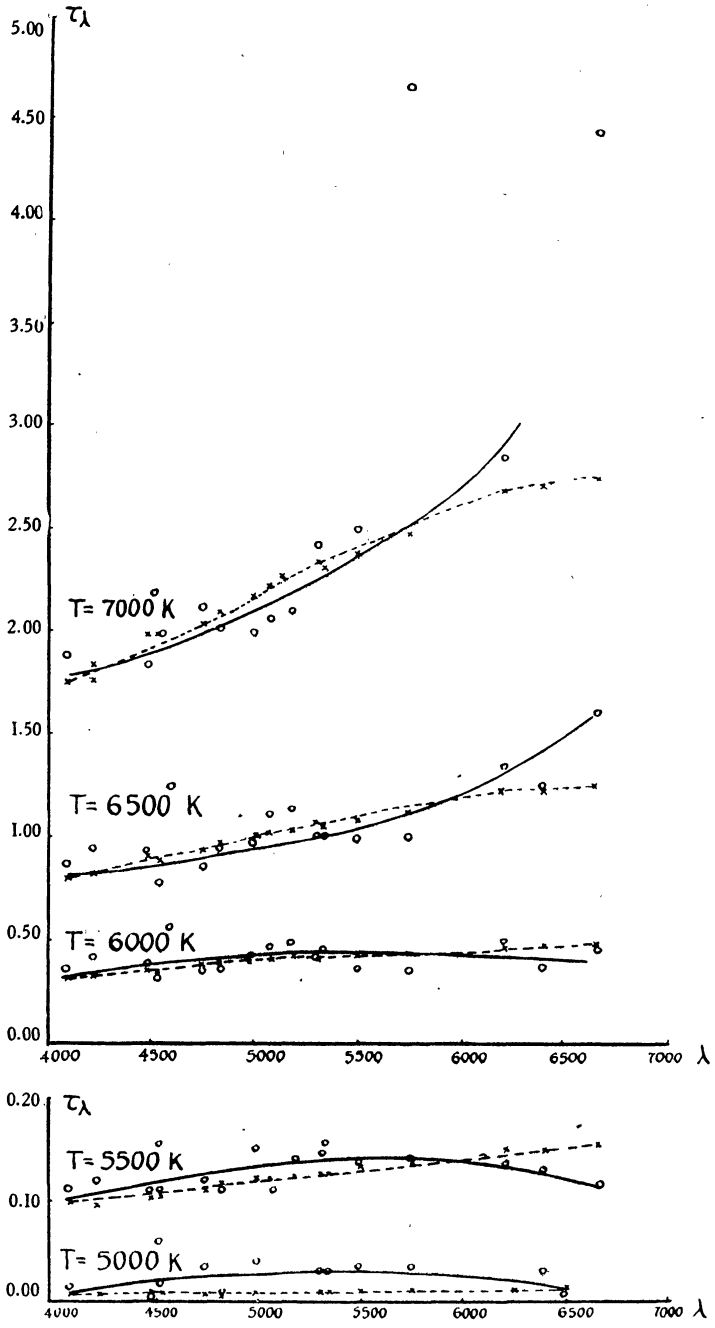

FIG. 2. — Variation of $\tau\lambda$ with λ for a few typical temperatures. Solid curves represent empirical τ_λ's computed from the observed limb darkening and Mulders' intensity distribution for the centre of the disc.

Broken curves represent synthetic τ_λ's obtained from the graphical integration of equation (11) using. Chandrasekhar's absorption coefficients for H^- ion and Mulders' intensity distribution for the centre of the disc.

and observation is already beginning to show up. However without extending the limb darkening observations further towards the longer wavelengths and at the same time determining more accurate values of absolute intensity at the centre of the disc, it is impossible to say whether this divergence is genuine.

VARIATION OF TEMPERATURE WITH OPTICAL DEPTH FOR 5 000 Å

It is usual to characterise the opacity of the photosphere by a relation between the temperature and the optical depth for the wavelength 5 000 Å.

We have determined this relation by graphically integrating the expression

$$\tau_\lambda(T) = \int_{4\,800}^{T} a_T k_\lambda(T) dT$$

for various temperatures for the wavelength 5 000 Å. A graph is drawn (see fig. 3) representing the variation of optical depth with temperature for this wavelength.

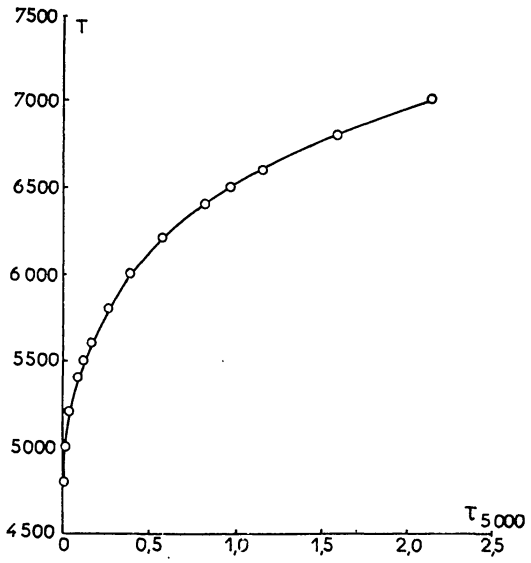

FIG. 3. — Variation of temperature with optical depth for $\lambda = 5\,000$ Å.

In conclusion, my sincere thanks are due to Dr. A. K. DAS, Director of this observatory for suggesting this problem to me and for giving me all facilities and guidance throughout the course of this investigation. Thanks are also due to Mr. K. D. ABHYANKAR for assistance in computations and to Mr. P. MADHAVAN NAYAR for suitably preparing the diagrams for the press.

Manuscrit reçu le 20 *décembre* 1953.

RÉFÉRENCES

[1] ABBOT, *Ann. Smiths. Instit.*, **3**, 1913, 159 ; **4**, 1922, 220. — MOLL, BURGER, VAN DER BILT, *B. A. N.*, **3**, 1925, 83. — RAUDENBUSCH, *A. N.*, **266**, 1938, 316. — CANAVAGGIA and CHALONGE, *Ann. Ap.*, **9**, 1946, 143. — MINNAERT, VAN DEN HOVEN, VAN GENDEREN and J. VAN DIGGELEN, *B. A. N.*, **11**, 1949, 55. — PIERCE, Mc MATH GOLDBERG and MOHLER, *Ap. J.*, **112**, 1950, 289. — PEYTURAUX, *Ann. Ap.*, **15**, 1952, 302.

[2] R. CANAVAGGIA and D. CHALONGE, *Ann. Ap.*, **9**, 1946, 143.

[3] D. CHALONGE and V. KOURGANOFF, *Ann. Ap.*, **9**, 1946, 69.

[4] R. WILDT, *Ap. J.*, **89**, 1939, 295 ; also *Ap. J.*, **90**, 1939, 611.

[5] S. CHANDRASEKHAR and G. MÜNCH, *Ap. J.*, **104**, 1946, 446.

[6] A. K. DAS and A. S. RAMANATHAN, *Zs. f. Ap.*, **32**, 1953, 91-103.

[7] M. MINNAERT, *B. A. N.*, **11**, 1949, 55.

[8] A. J. M. WANDERS, *Zs. f. Ap.*, **8**, 1934, 108.

[9] V. KOURGANOFF, *C. R.*, **228**, 1949, 2011.

[10] V. KOURGANOFF, *Basic Methods in Transfer Problems*, Cambridge, 1953, p. 266.

[11] S. CHANDRASEKHAR and F. BREEN, *Ap. J.*, **104**, 1946, 444.